

## REVIEW / SYNTHÈSE

**NMR methods for the study of protein structure and dynamics****Lewis E. Kay**

**Abstract:** An understanding of the role played by a protein in cellular function requires a detailed picture of its three-dimensional structure as well as an appreciation of how the structure varies as a function of time as a result of molecular dynamics. Over the past several years, multidimensional, multinuclear solution NMR spectroscopy has become a powerful technology for obtaining both structural and dynamical information on proteins and protein-ligand systems. In the present review, a number of new methodological advances are highlighted that have significantly improved the quality of NMR spectra of biomolecules and have increased the molecular weight limitations previously imposed on NMR-based structural studies of macromolecules. Applications of this technology to a number of protein systems currently studied in my laboratory are presented.

**Key words:** nuclear magnetic resonance, NMR, protein structure, protein dynamics, protein thermodynamics, Src homology 2 domain, SH2.

**Résumé :** La compréhension du rôle que joue une protéine dans la fonction des cellules nécessite une étude détaillée de sa structure tridimensionnelle, ainsi qu'une appréciation de la variation de sa structure en fonction du temps à cause de la dynamique moléculaire. Au cours des dernières années, la spectroscopie de résonance magnétique nucléaire (RMN) multidimensionnelle et multinucléaire en solution est devenue une technique puissante pour obtenir des informations sur la dynamique et la structure des protéines et des complexes protéine-ligand. Cette revue fait le point sur divers nouveaux progrès méthodologiques qui ont amélioré significativement la qualité des spectres de RMN des molécules biologiques et ont diminué les limites antérieures imposées par la masse moléculaire qui restreignait les études de la structure des macromolécules à l'aide de la RMN. Des applications de cette technologie à l'étude de divers systèmes protéiques dans mon laboratoire sont présentées.

**Mots clés :** résonance magnétique nucléaire, RMN, structure protéique, dynamique protéique, thermodynamique protéique, domaine 2 homologue à Src, SH2.

[Traduit par la rédaction]

**Introduction**

In the past decade NMR spectroscopy has emerged as a powerful technique for the determination of the three-dimensional structures of proteins in solution. In the early 1980s, studies by R.R. Ernst (described in Ernst et al. 1987) and K. Wüthrich (1986) demonstrated that it is possible to obtain atomic resolution structures of small proteins, with molecular masses less than approximately 10 kDa (100 amino acids). The work of

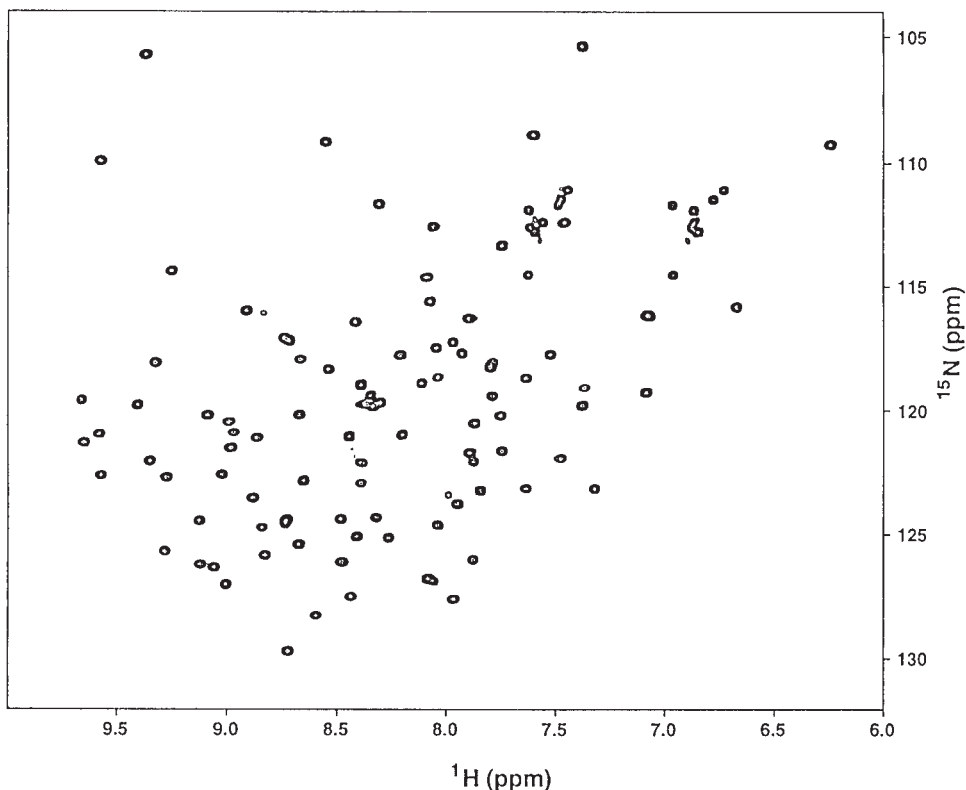
Ernst provided the framework for the extension of the NMR technique from one to two and three frequency dimensions. Recent developments in NMR spectroscopy have had a further significant impact on solution structural studies of proteins (Bax 1994; Kay 1995a). The improvements in the technology have been severalfold and include (*i*) the increase in the dimensionality of experiments from two to three and four, providing improved resolution for complex spectra; (*ii*) the

Received December 9, 1996. Accepted January 30, 1997.

**Abbreviations:** CBCA(CO)NH,  $\alpha/\beta$  carbon (via carbonyl carbon) to nitrogen to amide proton correlation; CT, constant time; CT-HNCA, constant time acquisition amide proton to nitrogen to  $\alpha$  carbon correlation; CT-HN(CO)CA, constant time amide proton to nitrogen to  $\alpha$  carbon (via carbonyl carbon) correlation; CT-HN(COCA)CB, constant time amide proton to nitrogen to  $\beta$  carbon (via carbonyl carbon and  $\alpha$  carbon) correlation; HCCH-TOCSY, proton-carbon-carbon-proton correlation using carbon total correlation spectroscopy; HNCACB, amide proton to nitrogen to  $\alpha/\beta$  carbon correlation; HSQC, heteronuclear single quantum coherence; *n*D, *n*-dimensional; NMR, nuclear magnetic resonance; NOE, nuclear Overhauser effect; ns, nanosecond; PLCC, C-terminal SH2 domain from phospholipase C $\gamma$ 1; ps, picosecond; pTyr, phosphotyrosine; pY1009, tyrosine-phosphorylated peptide from the tyrosine-1009 site of the platelet-derived growth factor receptor; pY1021, tyrosine-phosphorylated peptide from the tyrosine-1021 site of the platelet-derived growth factor receptor; RNase HI, *Escherichia coli* ribonuclease HI; SH2, Src homology 2 domain.

**L.E. Kay.** Departments of Medical Genetics, Biochemistry, and Chemistry, University of Toronto, Toronto, ON M5S 1A8, Canada.

**Fig. 1.**  $^1\text{H}$ - $^{15}\text{N}$  HSQC spectrum recorded on a 1 mM, uniformly  $^{15}\text{N}$ -labeled sample of PLCC SH2 in a 1:1 complex with pY1021 peptide. The sample was dissolved in 90%  $\text{H}_2\text{O}$ , 10%  $\text{D}_2\text{O}$ , pH 6.0, and 0.1 M sodium phosphate, 30°C. The spectrum was recorded at 500 MHz ( $^1\text{H}$  frequency). Reproduced with permission from Kay (1995b).



uniform incorporation of  $^{15}\text{N}$ ,  $^{13}\text{C}$ , and  $^2\text{H}$  labels into the biological system of interest coupled with the development of sophisticated NMR pulse schemes to transfer magnetization between scalar (through bond) and dipolar (through space) coupled spins; and (iii) significantly improved radio frequency (RF) electronics and increased magnetic field strengths as well as the development of commercially available hardware such as pulsed field gradients. Using this technology, a large number of structures of proteins or protein complexes in the molecular mass range of 15–20 kDa have been reported in the past several years (Ikura et al. 1992; Zhang et al. 1994) and applications to systems in the 30–40 kDa range are underway. Recently, the backbone assignments for a 64 kDa ternary complex of a tandem dimer of trp-repressor and operator DNA have been reported (Shan et al. 1996).

### Chemical shift assignment: the first step

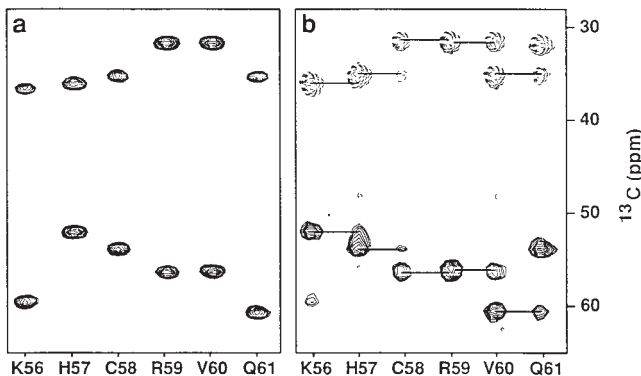
The first step in any NMR study of molecular structure or dynamics is to assign the frequencies at which energy absorption occurs for each of the specific NMR active nuclei in the sample under investigation. The frequency of absorption is directly related to a parameter termed chemical shift and a large number of experiments have been developed in the past two decades for chemical shift assignment. In many respects the chemical shift of a particular nucleus can be thought of as its “nuclear signature” and once such information is available the spectroscopist has a handle on probing structure and dynamics at that site in the molecule. Because macromolecules

contain many NMR active nuclei, there is often a large degree of overlap in 1 and 2D NMR spectra and recourse to higher dimensionality experiments is necessary. It is beyond the scope of the present article to describe all of the available methods for obtaining the necessary resolution so that a complete set of chemical shifts can be obtained. Rather, methods that my laboratory has been actively involved in developing over the past 5 years are highlighted.

### Triple resonance NMR spectroscopy

Many of the modern NMR methods for studying proteins in excess of 100 amino acids make use of uniform  $^{15}\text{N}$  and  $^{13}\text{C}$  labeling and are called triple resonance ( $^1\text{H}$ ,  $^{15}\text{N}$ ,  $^{13}\text{C}$ ) techniques because the naturally present  $^1\text{H}$  resonances of the molecule are recorded along with those of incorporated  $^{15}\text{N}$  and  $^{13}\text{C}$  nuclei. Triple resonance methods exploit the large couplings that exist between the  $^{15}\text{N}$  and  $^{13}\text{C}$  nuclei and between these nuclei and their directly attached protons for efficient magnetization transfer. In this approach, assignment of backbone  $^{15}\text{N}$ , NH,  $^{13}\text{C}^\alpha$ ,  $^{13}\text{C}^\beta$ ,  $^{13}\text{C}'$  (carbonyl),  $^1\text{H}^\alpha$ , and  $^1\text{H}^\beta$  chemical shifts is accomplished using 3D experiments that correlate nuclei three at a time. Because of their excellent resolution and sensitivity and the redundancy of information, backbone assignment is straightforward. Figure 1 illustrates a 2D  $^1\text{H}$ - $^{15}\text{N}$  heteronuclear single quantum correlation spectrum recorded on a 1-mM sample of a 105 amino acid fragment comprising the C-terminal SH2 domain from phospholipase C $\gamma$ 1 (PLCC) in 1:1 complex with a 12 residue target phosphorylated

**Fig. 2.** Strip plots from (a) CBCA(CO)NH and (b) HNCACB data sets recorded at 500 MHz on a 1.5 mM  $^{15}\text{N}$ ,  $^{13}\text{C}$ -labeled PLCC SH2 sample (90%  $\text{H}_2\text{O}$ , 10%  $\text{D}_2\text{O}$ , pH 6.0, 0.1 M sodium phosphate, 30°C) in a 1:1 complex with pY1021 peptide. Correlations involving amides of residues Lys 56 to Gln 61 are illustrated. Reproduced with permission from Kay (1995b).



peptide, pY1021, from the tyrosine-1021 site of the platelet-derived growth factor receptor. This spectrum is particularly useful in that it records the  $^{15}\text{N}$  and NH chemical shifts of all backbone and sidechain NH positions in the molecule.

An example of the utility of the triple resonance approach is provided in Fig. 2, where slices from each of the CBCA(CO)NH and HNCACB spectra of the PLCC SH2 domain are illustrated. The CBCA(CO)NH experiment provides correlations linking the  $^{13}\text{C}^\beta$  and  $^{13}\text{C}^\alpha$  chemical shifts of a residue with the  $^{15}\text{N}$  and NH chemical shifts of the sequential residue. In contrast, the HNCACB links both intraresidue and interresidue  $^{13}\text{C}^\beta$  and  $^{13}\text{C}^\alpha$  chemical shifts with ( $^{15}\text{N}$ , NH) spin pairs. In some cases, these two experiments are sufficient to obtain the backbone NH,  $^{15}\text{N}$ ,  $^{13}\text{C}^\alpha$ , and  $^{13}\text{C}^\beta$  chemical shift assignment. For most proteins, however, additional experiments must be performed.

Sidechain assignments use the 3D HCCH-TOCSY as well as experiments correlating sidechain  $^1\text{H}$  and  $^{13}\text{C}$  shifts with backbone  $^{15}\text{N}$  and NH shifts (Bax 1994). Figure 3 illustrates a gradient HCCH-TOCSY developed in my laboratory that can be recorded on samples dissolved in  $^1\text{H}_2\text{O}$  as solvent. Because of the proximity of many of the aliphatic sidechain resonances to the water signal, pulsed field gradient technology, discussed below, has been used to eliminate the water signal, while retaining the spectrum of the protein. The excellent water suppression capabilities associated with this method are illustrated in the figure. Finally, structural information is obtained from nuclear Overhauser effect (NOE) experiments that provide distance correlations between protons within 5 Å of each other. We have developed an experiment that allows the simultaneous recording of  $^{15}\text{N}$ - and  $^{13}\text{C}$ -edited NOE spectra of uniformly  $^{15}\text{N}$ - and  $^{13}\text{C}$ -labeled proteins dissolved in  $\text{H}_2\text{O}$  (Pascal et al. 1994a). The experiment is particularly useful in that each NOE benefits from having a symmetry related partner in the spectrum, facilitating the assignment of NOE peaks to particular pairs of protons. This is illustrated in Fig. 4 where a number of slices from a 150 ms mixing time simultaneous  $^{15}\text{N}$ - and  $^{13}\text{C}$ -edited NOESY HSQC data set recorded on a 1.5 mM PLCC SH2 sample are shown. Note the symmetry related cross peaks linking Leu 80 NH and Leu 77  $\text{H}^\alpha$  as well as Met 26 NH and Ile 55  $\text{H}^\delta$ .

## Pulsed field gradient NMR

It has long been recognized by NMR spectroscopists that the application of magnetic field gradients in an NMR experiment could act as a filter by selecting magnetization having desired properties while rejecting all other magnetization components (Keeler et al. 1994 and references therein). This selection process can be understood by noting that the application of a magnetic field gradient imparts a phase shift on the magnetization, the amplitude of which is dependent on the position of the resonating nuclei in the magnetic field, the duration and strength of the field gradient, and the nuclei in question ( $^1\text{H}$ ,  $^{13}\text{C}$ ,  $^{15}\text{N}$ ,  $^{31}\text{P}$ , etc.). By applying a second field gradient at some time later in the pulse sequence and by judiciously choosing the strength and (or) duration of this gradient pulse, the phase shift imparted by the first gradient pulse is refocussed. The phase shifts associated with “unwanted” components of magnetization are not refocussed, however, and would-be artifacts in spectra can be eliminated. An alternative strategy for elimination of artifactual signals is to leave the magnetization of interest intact and to use gradients to suppress the signals that are not of interest directly. Both methods provide spectra of high quality.

The suppression of signals that are not of interest by the application of pulsed field gradients can be accomplished in a single scan. In contrast, in the absence of pulsed field gradients, experimental artifacts are eliminated by repeating the NMR experiment several times with different phases for particular pulses in the pulse sequence. The resulting signals are added so that real signals grow in intensity and unwanted magnetization components cancel. This process, called phase cycling, requires very high spectrometer stability, often for a time period of days. In complex NMR experiments, artifacts are often incompletely suppressed because of limitations imposed by spectrometer stability as well as the use of incomplete phase cycling schemes. It is clear that gradient technology offers far superior performance relative to the more traditional approach based on phase cycling.

Despite the advantages of using pulsed field gradients to select for the signals of interest in NMR experiments, many of the early applications resulted in a sensitivity loss of factors of at least 2 and often larger. These sensitivity losses arise because in many experiments the use of gradients naturally selects only one of two possible pathways of magnetization transfer, although in non-gradient experiments both magnetization pathways contribute to the observed signal. Both my laboratory and the laboratory of Christian Griesinger have recently developed methods that use gradients to select for transfer pathways that do not suffer from sensitivity losses whatsoever (Kay et al. 1992; Schleucher et al. 1993; Muhandiram and Kay 1994; Schleucher et al. 1994).

## Development of $^{15}\text{N}$ , $^{13}\text{C}$ , $^2\text{H}$ NMR spectroscopy

As discussed above,  $^1\text{H}$ ,  $^{13}\text{C}$ ,  $^{15}\text{N}$  triple resonance 3D and 4D spectroscopy has increased the size limits of protein structures that can be determined by the NMR technique to about 25 kDa. There are two reasons for this limit. First, as the molecular weight increases, the number of cross peaks in spectra also increases. In the case of the triple resonance experiments developed for backbone assignment, the number of peaks

**Fig. 3.**  $^1\text{H}$ - $^1\text{H}$  slices of the gd-HCCH-TOCSY spectrum of 2.2 mM  $^{15}\text{N}$ ,  $^{13}\text{C}$ -labeled PLCC SH2 dissolved in 90%  $\text{H}_2\text{O}$ , 10%  $\text{D}_2\text{O}$ , pH 6.0, and 0.1 M sodium phosphate, 30°C. No presaturation or postacquisition data massaging to remove the residual water was used. Reproduced with permission from Kay (1995b).

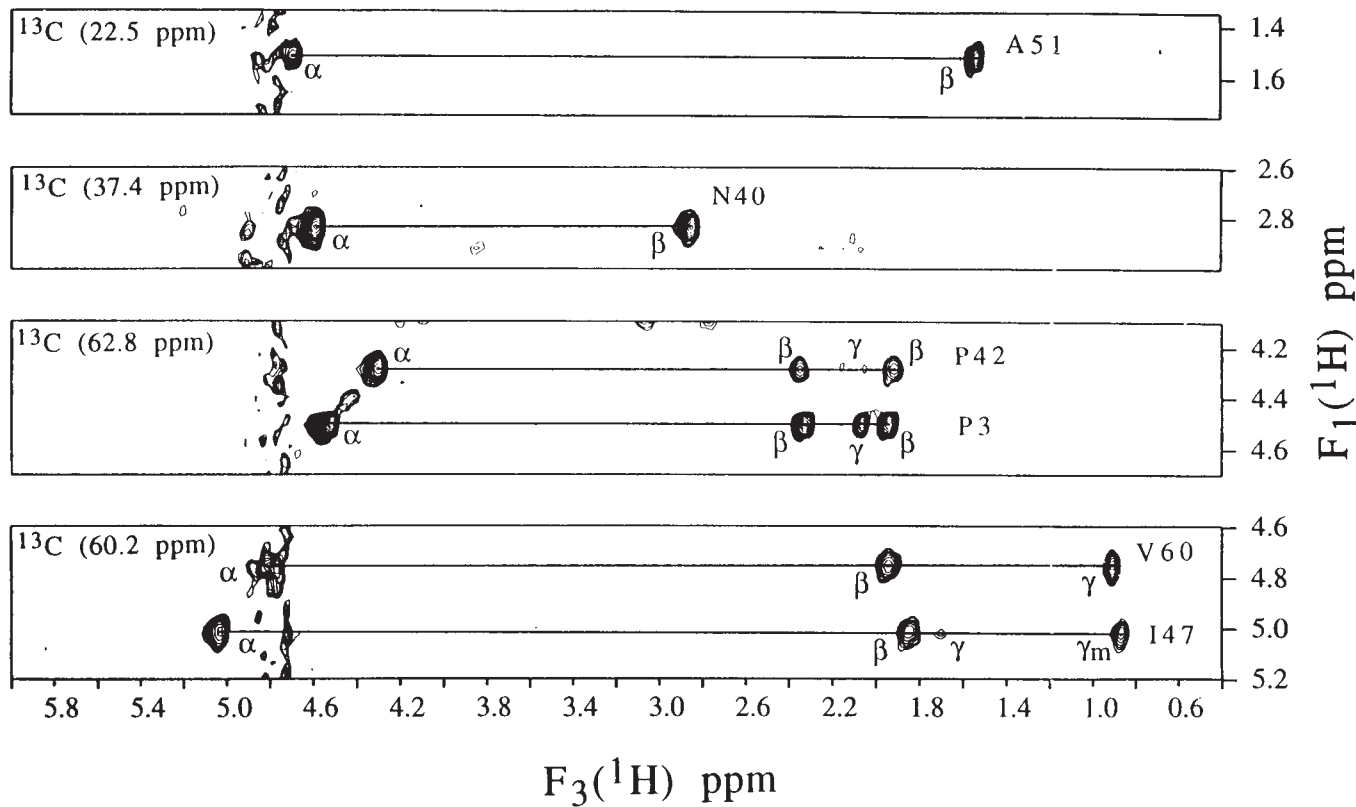
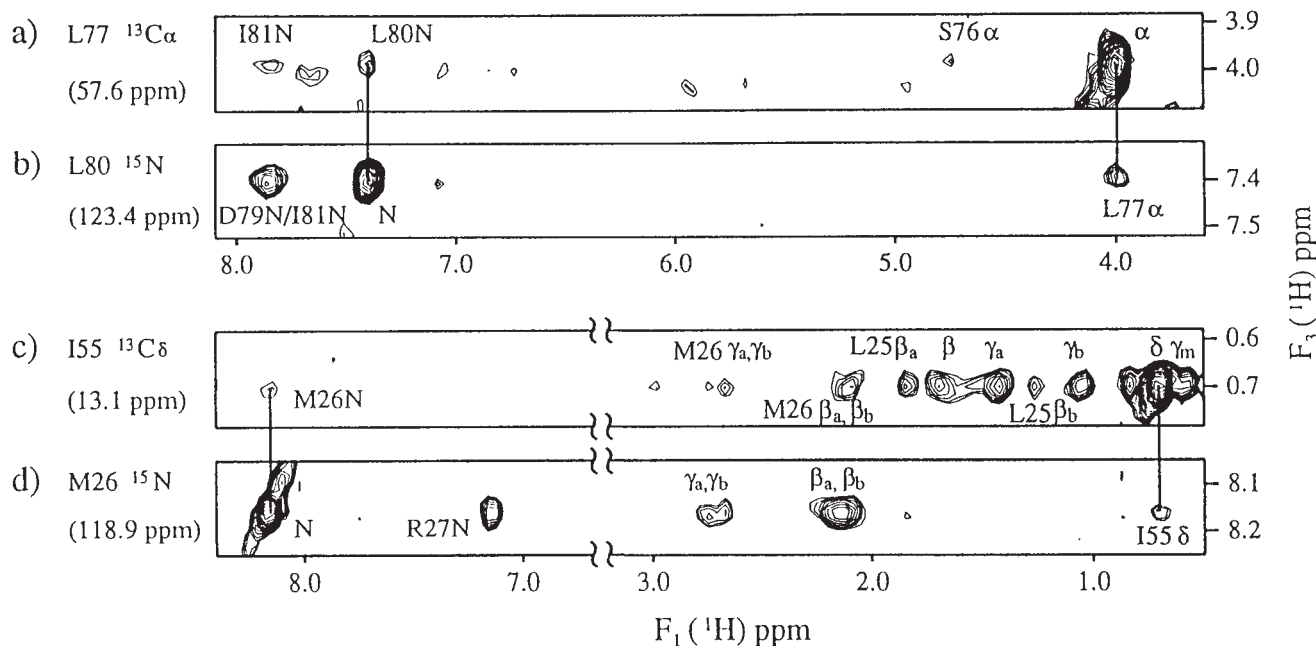
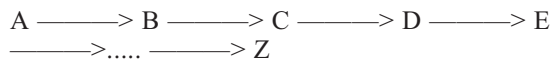


**Fig. 4.** Slices from a 150 ms mixing time simultaneous  $^{15}\text{N}$ -edited and  $^{13}\text{C}$ -edited NOESY-HSQC data set recorded on a sample of 1.5 mM  $^{15}\text{N}$ ,  $^{13}\text{C}$ -labeled PLCC SH2 (90%  $\text{H}_2\text{O}$ , 10%  $\text{D}_2\text{O}$ , pH 6.0, 0.1 M sodium phosphate, 30°C) in a 1:1 complex with pY1021 peptide. Symmetry related cross peaks showing correlations between (a, b) Leu 80 NH and Leu 77 H $^\alpha$  and (c, d) Met 26 NH and Ile 55 H $^\delta$  are highlighted. Reproduced with permission from Pascal et al. (1994b).



increases in a linear fashion with molecular weight. The number of cross peaks in NOE-type spectra also increases rapidly with size and poses a serious problem for studying larger proteins. However, the rapid decay of the NMR signal that occurs during the multitude of transfer steps in a complex NMR experiment has the most significant effect on the size of molecules that can be studied by NMR. A typical multidimensional NMR experiment can be schematized as follows:

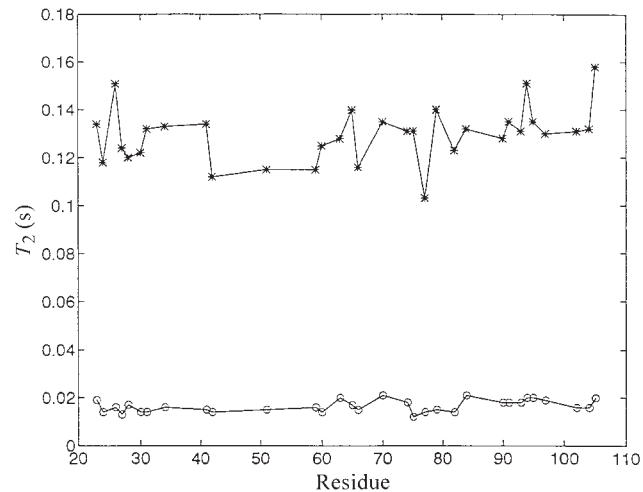


where the transfer of magnetization proceeds from A to Z via B, C, D, etc. The amount of time required to transfer magnetization along each link in the chain, for example from B to C, is a function of the strength of the coupling between the participating links. The transfer can vary from 4 ms if B =  $^1\text{H}$  and C =  $^{13}\text{C}$  to 20–30 ms if B =  $^{15}\text{N}$  and C =  $^{13}\text{C}$ , for example. During this transfer, the signal decays via relaxation processes in which efficiency, for macromolecules, increases linearly with molecular weight. The decay time of the signal varies depending on the type of nucleus (i.e., whether A =  $^1\text{H}$ ,  $^{13}\text{C}$ ,  $^{15}\text{N}$  etc); for  $^{13}\text{C}$  nuclei coupled to protons, the decay time can be as short as 15 ms for proteins in the 20–30 kDa range. If the decay rate is the same order of magnitude as the transfer rate, a significant attenuation of the signal can be expected. In principle, there are three approaches to increasing the amount of signal observed at the end of the transfer. The first is to increase the inherent sensitivity of the experiment. The enhanced sensitivity pulsed field gradient methodology that we have developed (Kay et al. 1992, discussed above) is an example of this class of experiment. The second is to increase the strength of the coupling between the spins involved in the transfer. Unfortunately, these couplings are fixed by spin type and can not be manipulated. The third approach is to decrease the efficiency of relaxation loss that occurs during the transfer. This can be manipulated experimentally through the substitution of deuterium for carbon-bound protons in the protein (Grzesiek et al. 1993; Yamazaki et al. 1994a, 1994b).

The relaxation of nuclei is caused by fluctuating magnetic fields that are the result of the overall molecular tumbling in solution as well as internal dynamics. For the case of heteronuclei such as  $^{15}\text{N}$  or  $^{13}\text{C}$  directly coupled to  $^1\text{H}$  spins, the major source of relaxation is due to fluctuating dipolar fields caused by the  $^1\text{H}$  spins. The sizes of these dipolar fields are proportional to the gyromagnetic ratio of the spins that give rise to the fields, in this case  $^1\text{H}$  spins. By substituting  $^{13}\text{C}$ -bound protons with deuterons, the size of the dipolar fields that cause relaxation of the attached  $^{13}\text{C}$  nucleus is reduced by a factor of ~6.5 because the gyromagnetic ratio of deuterons ( $^2\text{H}$ ) is ~6.5 times smaller than that of protons. This results in a substantial decrease in the relaxation rates of the  $^{13}\text{C}$  spins. In addition, the proton nuclei remaining in the molecule have much slower decay rates as well because many of the relaxation pathways that would normally involve adjacent protons are significantly attenuated by the incorporation of deuterium. Figure 5 illustrates the increase in the  $T_2$ s of  $^{13}\text{C}^\alpha$  carbons that occurs on substitution of deuterons for protons in the case of a 37 kDa protein – DNA complex. Note that large  $T_2$  values correspond to small line widths and allow the signal to be transferred between coupled nuclei in an efficient manner.

The idea of using  $^2\text{H}$  labeling of proteins as a means of

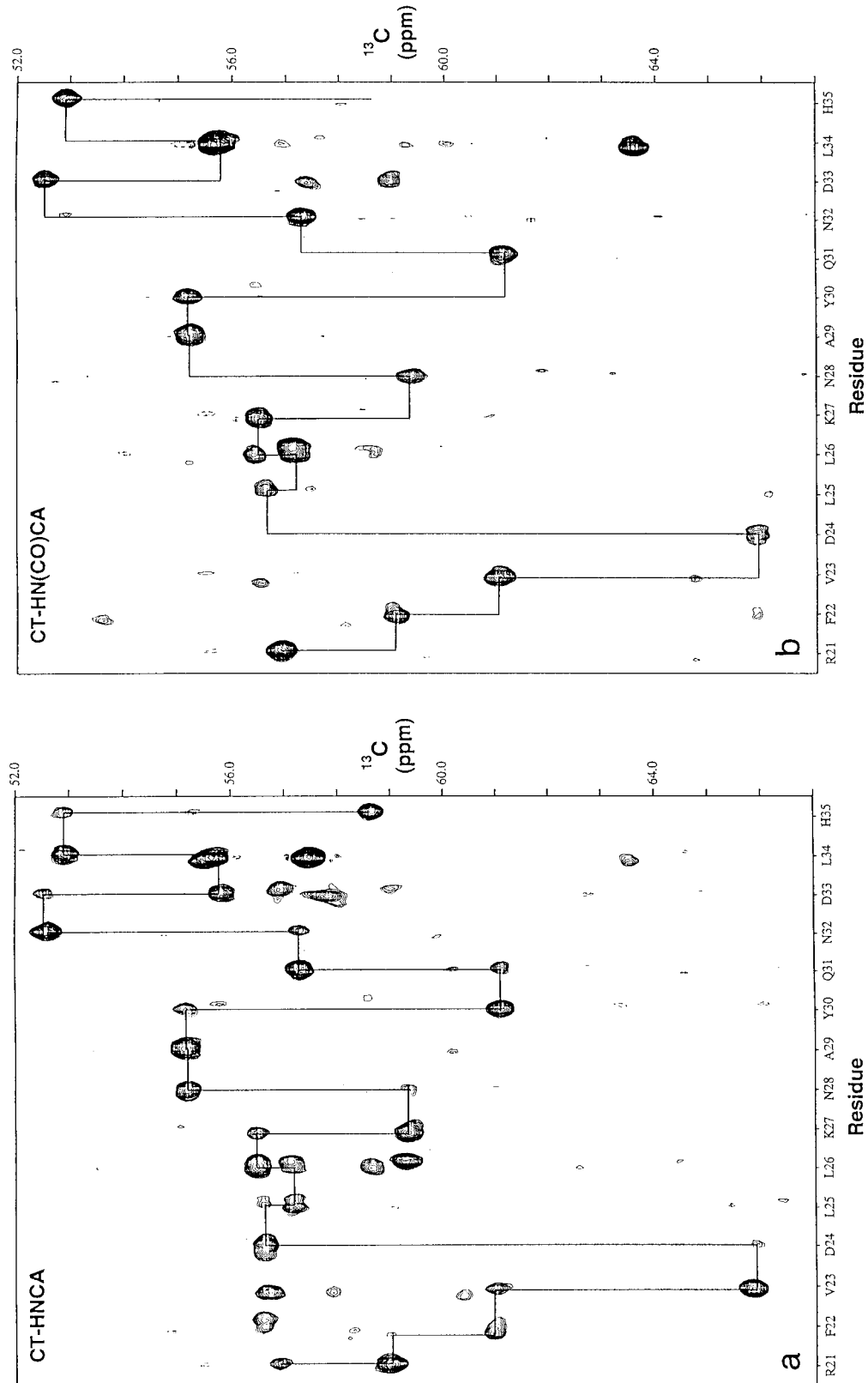
**Fig. 5.** Comparison of  $^{13}\text{C}^\alpha$  transverse relaxation times for  $^{13}\text{C}^\alpha-^2\text{H}^\alpha$  pairs (\*) vs.  $^{13}\text{C}^\alpha-^1\text{H}^\alpha$  pairs (o) in a ternary complex consisting of the  $^{15}\text{N}, ^{13}\text{C}$  labeled trp-repressor, fully protonated 5-methyltryptophan, and a fully protonated 20 basepair trp-operator DNA fragment. Average  $T_2$  values of 130 and 16.5 ms are obtained for the deuterated and protonated trp-repressor samples, respectively. Reproduced with permission from Yamazaki et al. (1994b).

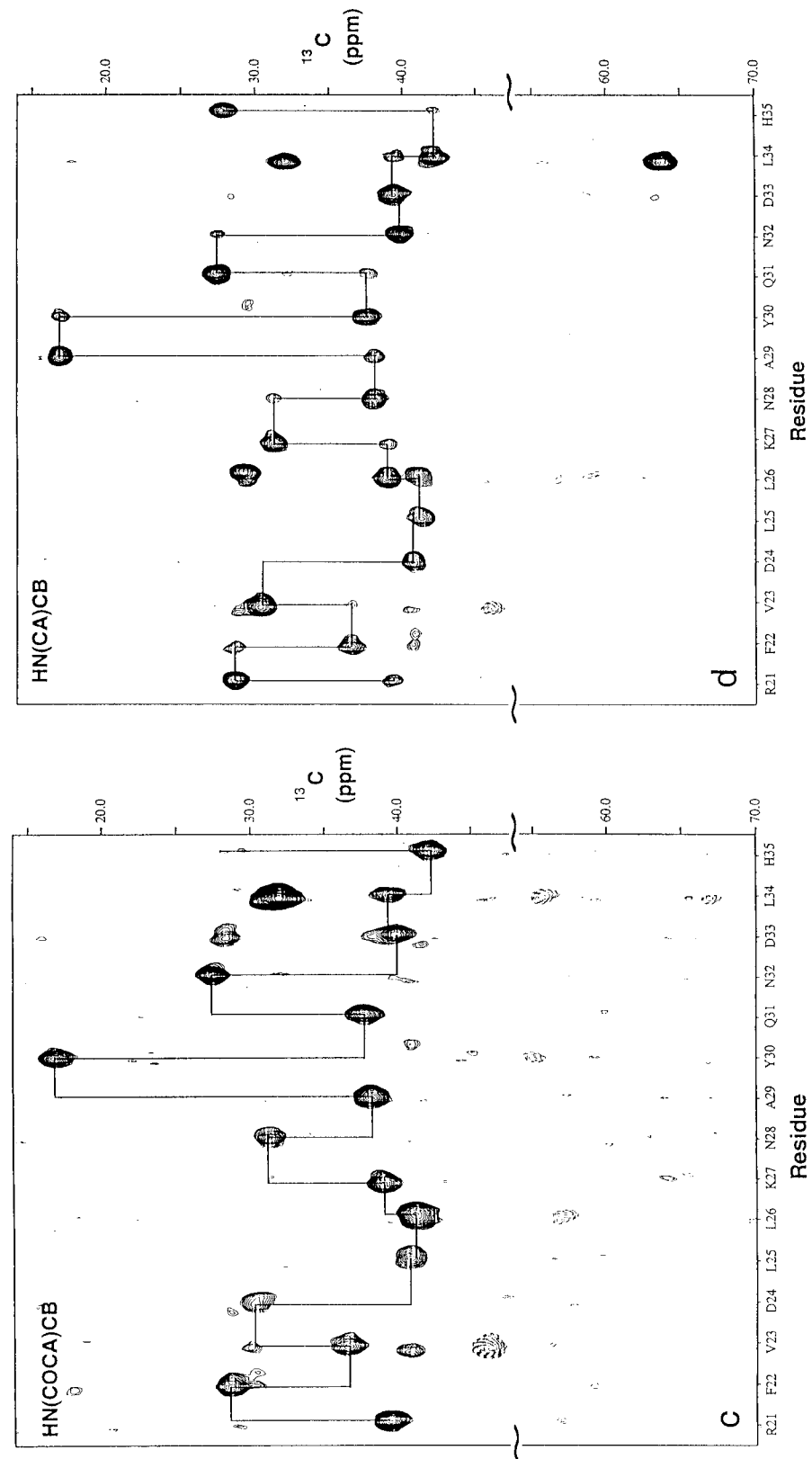


spectral editing dates back to the late 1960s with the pioneering experiments of Crespi et al. (1968) and Markley and co-workers (1968). In the late 1980s, the work of LeMaster (LeMaster and Richards 1988) demonstrated the utility of random fractional deuteration of proteins to aid in the sequential assignment of what was then considered to be a large protein for NMR studies, *Escherichia coli* thioredoxin (108 residues). The greatest impact of deuteration, however, is the combination of deuterium and  $^{15}\text{N}, ^{13}\text{C}$  labeling so that the triple resonance methods developed over the past several years can be extended to higher molecular weight systems. In this regard, we have recently developed a suite of triple resonance experiments for the backbone assignment of  $^{15}\text{N}, ^{13}\text{C}, ^2\text{H}$ -labeled proteins with high sensitivity and significantly improved resolution (Yamazaki et al. 1994a, 1994b). The methods have been applied to study the 37 kDa ternary complex of 100%  $^{15}\text{N}, ^{13}\text{C}$ - and ~70%  $^2\text{H}$ -labeled trp repressor, unlabeled co-repressor, and unlabeled trp operator DNA. The high sensitivity of the experiments is clearly illustrated in Figs. 6a–6d where sections from CT-HNCA, CT-HN(CO)CA, HN(COCA)CB, and HN(CA)CB 3D spectra are indicated. These spectra record  $^{15}\text{N}$ , NH, and either  $^{13}\text{C}^\alpha$  or  $^{13}\text{C}^\beta$  chemical shifts and, in the case of the 37 kDa complex considered here, the information content available from these spectra was sufficient for the complete backbone assignment. It is noteworthy that spectra were recorded in very reasonable measuring times (less than 2.5 days/spectrum) on a 2.4 mM sample at a field strength of 500 MHz.

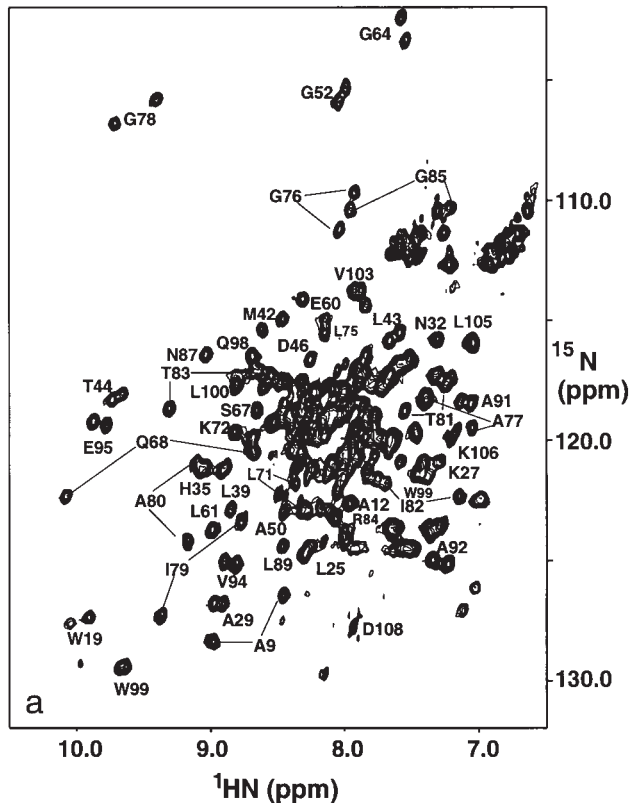
Our choice of a deuteration level of ~70% for the trp-repressor dimer complex was based on the intent that this sample would be used not only for sequential assignment but also for structural analysis. Therefore, in constructing this sample, we hoped to achieve a balance between a sufficiently high level of deuteration, with a concomitant increase in carbon relaxation times (see Fig. 5), and retaining an adequate supply

**Fig. 6.** (a) Strip plot showing the region of the CT-HNCA spectrum of the ternary trp-repressor complex ( $^{15}\text{N}$ ,  $^{13}\text{C}$ , ~70%  $^2\text{H}$  labeled trp-repressor, fully protonated 5-methyltryptophan, and a fully protonated 20 basepair trp-operator DNA) from Arg 21 to His 35. Both intraresidue and interresidue connectivities linking  $^{15}\text{N}$ ,  $^{13}\text{C}^\alpha$ , and NH shifts are obtained from this experiment. (b) Corresponding region of the CT-HN(CO)CA spectrum showing correlations connecting the  $^{15}\text{N}$ , NH chemical shifts with the  $^{13}\text{C}^\alpha$  shift of the preceding residue. (c) Strip plot of the HN(COCA)CB spectrum correlating the  $^{13}\text{C}^\beta(i-1)$ ,  $^{15}\text{N}(i)$ , and NH( $i$ ) chemical shifts of Arg 21 to His 35. (d)  $^{13}\text{C}^\beta(i)$ / $^{13}\text{C}^\beta(i-1)$ ,  $^{15}\text{N}(i)$ , and NH( $i$ ) correlations from the HN(CA)CB spectrum. The high sensitivity of each spectrum recorded on a 2 mM sample in about 2 days of measuring time is evident. Adapted from Yamazaki et al. (1994 b).



**Fig. 6 (concluded).**

**Fig. 7.** (a)  $^{15}\text{N}$ – $^1\text{H}$  correlation map of the 64 kDa tandem trpR complex, consisting of two trpR homodimers bound to a symmetrized operator DNA and stabilized by the co-repressor analog 5-methyl-L-tryptophan. Selected resonances are labeled illustrating the doubling of cross peaks observed for most of the residues.



of protons for the establishment of distance constraints via measurement of  $^1\text{H}$ – $^1\text{H}$  NOEs. Recent backbone assignment experiments carried out on a 64 kDa tandem trp-repressor complex in our laboratory were only possible when performed on a >90% deuterated  $^{15}\text{N}$ ,  $^{13}\text{C}$ -labeled sample, stressing the requirement for high levels of deuteration for the study of large molecular weight proteins and protein–ligand complexes (Shan et al. 1996). Figure 7 illustrates the  $^1\text{H}$ – $^{15}\text{N}$  correlation map of the 64 kDa trp-repressor complex and sections from 3D CT-HNCA, CT-HN(CO)CA, CT-HN(CA)CB, and CT-HN(COCA)CB experiments. These experiments correlate NH and  $^{15}\text{N}$  spin pairs with intraresidue and interresidue  $^{13}\text{C}^\alpha$ / $^{13}\text{C}^\beta$  shifts (CT-HNCA/CT-HN(CA)CB) and interresidue  $^{13}\text{C}^\alpha$ / $^{13}\text{C}^\beta$  shifts (CT-HN(CO)CA/CT-HN(COCA)CB).

Although such a perdeuteration scheme is of benefit for the assignment of backbone NH,  $^{15}\text{N}$ , and  $^{13}\text{C}$  chemical shifts, the depletion of protons results in molecules with significant levels of protonation only at exchangeable NH sites. Structural studies by NMR depend to a large extent on the generation of interproton distance restraints, established via NOE-based experiments. The absence of large numbers of protons therefore poses a very serious problem for obtaining three-dimensional structures of proteins using current NMR approaches. With these limitations in mind, we have currently developed a bio-synthetic approach in which overexpression of proteins in  $\text{D}_2\text{O}$  and with protonated [ $^{13}\text{C}$ ]pyruvate as the sole carbon source

results in molecules that are highly deuterated at the majority of positions, with the exception of methyl groups of Ala, Val, Leu, and Ile ( $\gamma 2$ ) (Rosen et al. 1996). Our choice of methyl groups as sites of protonation in otherwise largely perdeuterated molecules is based on a number of factors. First, methyl proton and carbon chemical shifts show a reasonably high degree of dispersion in  $^1\text{H}$ – $^{13}\text{C}$  correlation spectra. In addition, rapid rotation about the methyl symmetry axis leads to significantly narrowed [ $^{13}\text{C}$ ] and [ $^1\text{H}$ ]methyl line widths, even in large proteins. For example, although the transverse relaxation of  $^{13}\text{C}$  magnetization is highly nonexponential in a methyl group, the slowly decaying components (which correspond to 75% of the signal in an isolated methyl spin system) have line widths of only a few Hertz, even for proteins of 40 kDa (Kay et al. 1992). In addition, the presence of multiple protons per methyl group ensures that efficient longitudinal relaxation of the methyl protons can occur via intra-methyl dipolar interactions, even in proteins with high levels of deuteration at other positions (Gardner et al. 1996a). It is therefore possible to acquire spectra in reasonably short measuring times. Finally, statistical studies of high resolution X-ray derived structures show that Ala, Val, Leu, and Ile are among the most highly represented amino acids in protein hydrophobic cores and at protein–protein interfaces (Janin et al. 1988). Thus, it seemed likely that the protons provided by these methyl groups would generate large numbers of distance restraints in the form of  $^1\text{H}$ – $^1\text{H}$  NOEs, allowing the establishment of protein global folds. Figure 8 illustrates the distribution of protons within the PLCC SH2 domain for a fully protonated sample, a sample where all carbon positions are deuterated and backbone amides are protonated and a sample in which methyl and backbone amide positions are protonated. It is clear that the addition of protonated methyl groups provides valuable structural probes.

The pathways involved in the production of Ala, Val, Leu, and Ile are illustrated in Fig. 9. Extensive NMR analysis and mass spectroscopic studies have established that the probability of an individual residue containing only deuterium at all carbon sites between the protonated methyl groups and the  $\text{C}^\alpha$  position is about 100, 98, 90, and 99% for Ala, Val, Leu, and Ile, respectively (Rosen et al. 1996). Because of the high levels of deuteration at most non-methyl positions, molecules labeled in this way can be assigned in a straightforward manner using recently developed  $^{15}\text{N}$ ,  $^{13}\text{C}$ ,  $^2\text{H}$  NMR experiments. Moreover, it is possible to relay the signal from the protonated methyl groups to the backbone  $^{15}\text{N}$ , NH spins using experiments that we have derived so that the methyls can be readily sequentially assigned (Gardner et al. 1996a). Preliminary studies indicate that high quality spectra can be obtained at the very least for proteins in the 30–40 kDa range.

The most important feature of such  $^{15}\text{N}$ ,  $^{13}\text{C}$ ,  $^2\text{H}$ ,  $^1\text{H}$ ,  $^{13}\text{C}$ -labeled molecules, however, is that it is possible to obtain NH–NH, NH–methyl, and methyl–methyl NOEs in such systems to determine overall protein folds. Experimental results on the  $^{15}\text{N}$ ,  $^{13}\text{C}$ ,  $^2\text{H}$ ,  $^1\text{H}$ ,  $^{13}\text{C}$ -labeled PLCC SH2 domain and calculations performed on a number of proteins ranging in molecular mass from 15–40 kDa indicate that it will be possible to generate global folds of most proteins in this fashion (Gardner et al. 1996b). It is anticipated that these selectively methyl-protonated samples will have broad utility in NMR analyses of high molecular weight species, ranging from the determination of global folds to the generation of models of multiprotein complexes.

**Fig. 7.** (b) Strip plot of CT-HNCA (black) and CT-HN(CO)CA (red) spectra showing  $^{13}\text{C}^\alpha(i)/^{13}\text{C}^\alpha(i-1)$ ,  $^{15}\text{N}(i)$ , and  $\text{NH}(i)$  chemical shift correlations for residues Asn 73 – Ala 80. The solid line shows the interresidue connectivity within one subunit and the dashed line shows the connectivity within the other. Peaks that are negative are indicated by the square boxes. Note that the correlations involving Gly 78 are folded once in the  $^{13}\text{C}^\alpha$  dimension. (c) Strip plot of CT-HN(CA)CB (black) and CT-HN(COCA)CB (red) spectra illustrating  $^{13}\text{C}^\beta(i)/^{13}\text{C}^\beta(i-1)$ ,  $^{15}\text{N}(i)$ , and  $\text{NH}(i)$  correlations extending from Asn 73 to Ala 80. Connectivities for the two subunits are distinguished by solid and dashed lines. The square boxes mark the peaks with negative phase. Adapted from Shan et al. (1996).

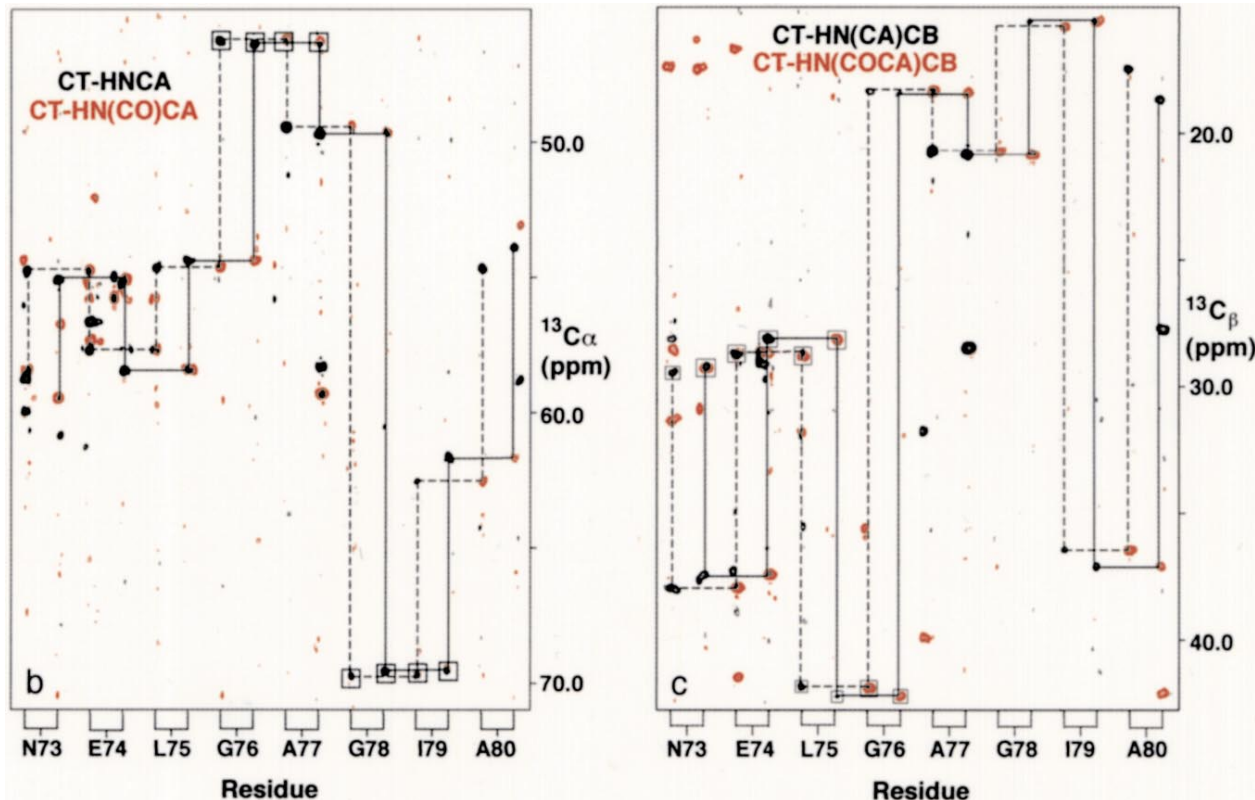


**Fig. 8.** (a) Distribution of all protons in the PLCC SH2 domain structure (Pascal et al. 1994b) from which  $^1\text{H}$ – $^1\text{H}$  distance restraints are derived. Protons are indicated by white (shaded) balls and the  $\text{C}^\alpha$  backbone trace is indicated in blue. (b) Remaining NH backbone protons after replacing all carbon-bound protons with  $^2\text{H}$ . (c) Distribution of NH and Ala, Val, Leu, and Ile ( $\gamma 2$  only) protons in PLCC SH2. The methyl protons are indicated in magenta.

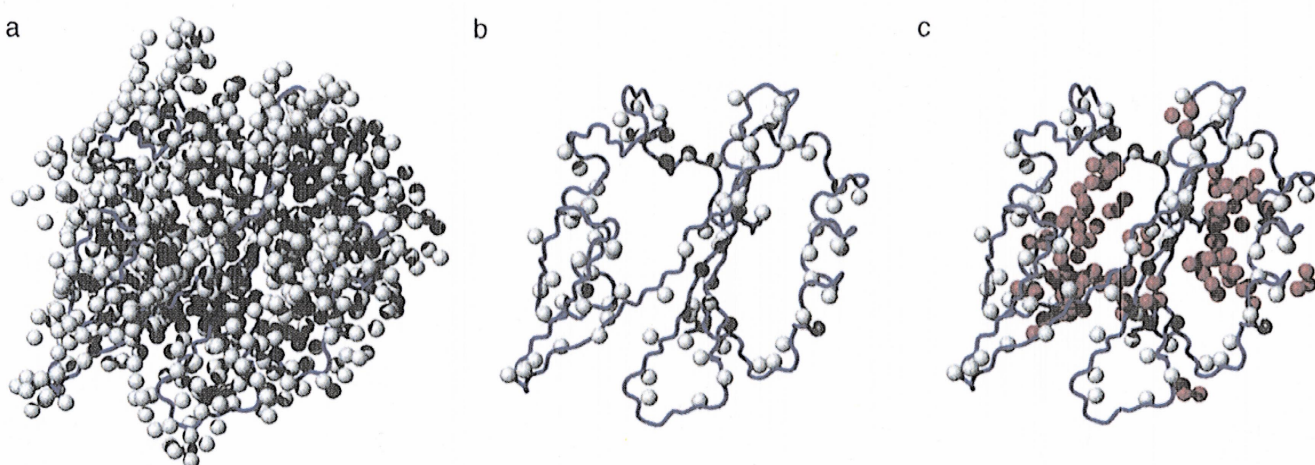


**Fig. 9.** Biosynthesis of Ala, Val, Leu, and Ile from pyruvate. The methyl groups of Ala, Leu, and Val are derived from pyruvate. The  $\gamma$ 2-methyl of Ile is derived from pyruvate, while the  $\delta$ -methyl is from Thr. Adapted from Rosen et al. (1996).

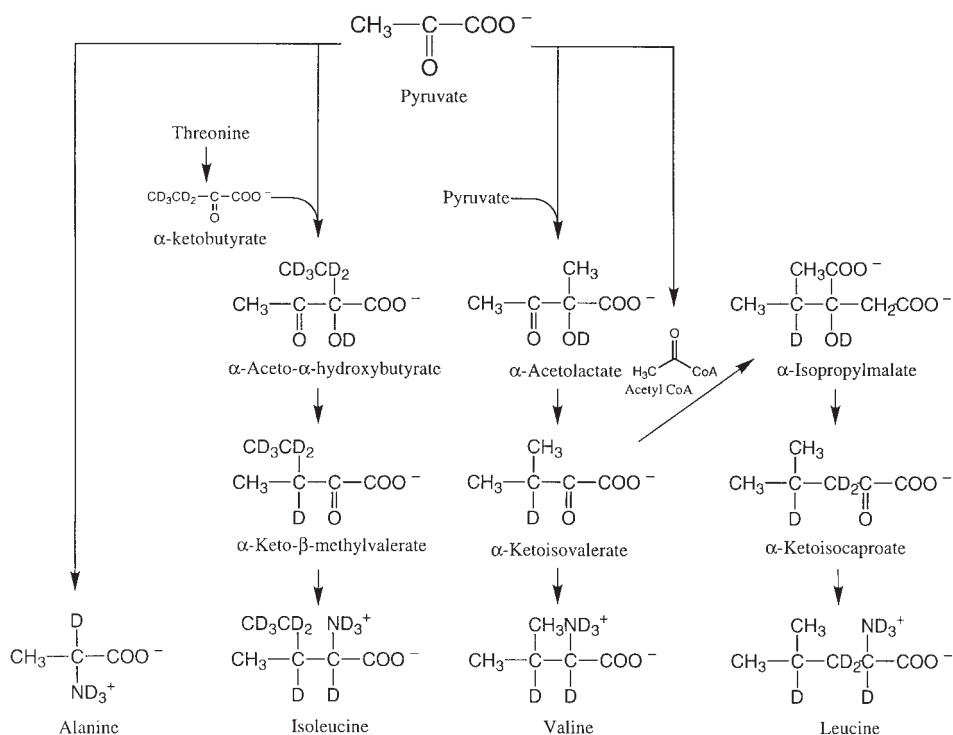
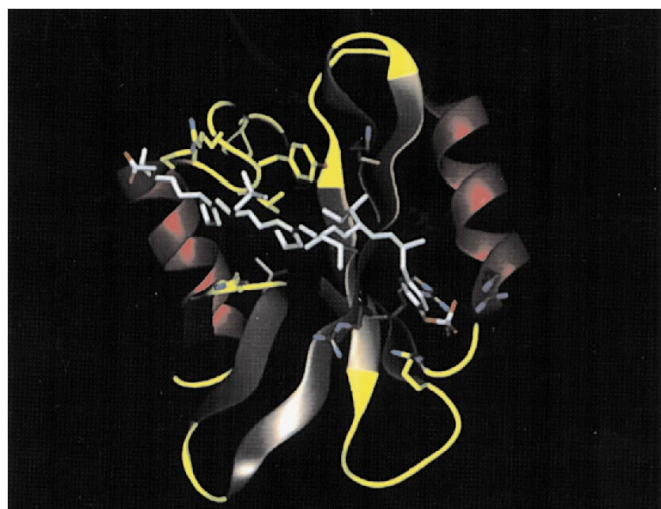


**Fig. 10.** Ribbon diagram of the solution NMR structure (Pascal et al. 1994b) of the PLCC SH2 domain in complex with the pY1021 peptide (white licorice bonds).

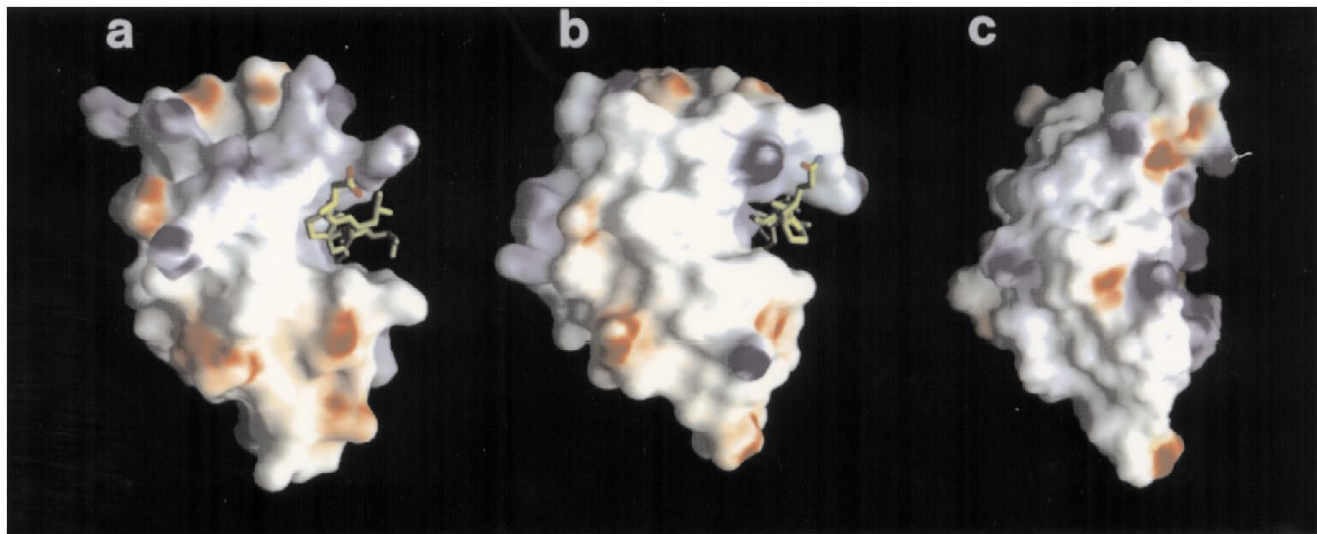


### Understanding protein dynamics

The identification of Src homology 2 (SH2) domains in many proteins involved in signal transduction has led to a rapid increase in our understanding of the molecular basis of oncogenesis. SH2 domains are regions of about 100 residues that

bind to specific phosphotyrosine (pTyr) containing sequences. Recently, the three-dimensional structures of a number of SH2 domains have been solved by nuclear magnetic resonance (NMR) and X-ray crystallographic methods (Yu and Schreiber 1994). These structural studies have revealed a similar overall topology for the SH2 domains consisting of a large central  $\beta$ -sheet and an associated  $\beta$ -sheet flanked by two  $\alpha$  helices. The phosphotyrosine binding site involves a network of charge-charge and hydrogen bonding interactions between residues of the SH2 domain, including arginine residues, and the phosphate oxygens and aromatic electrons of the pTyr ring from the peptide. In a collaboration between my laboratory and the laboratory of Julie Forman-Kay, the 3D solution structure of the PLCC SH2 domain in complex with pY1021 has been solved by heteronuclear NMR methods (Pascal et al. 1994b). Figure 10 illustrates the overall structure of the complex. The topology of this SH2-pTyr peptide complex is similar to that reported for the SH2 domains from Src (Waksman et al. 1992) and Lck (Eck et al. 1994). However, a striking difference between the structures is that in the case of the PLCC SH2 domain the binding site for residues C-terminal to the pTyr is an extended groove that contacts the peptide at residues extending from the pTyr to positions six residues C-terminal to the pTyr. In contrast, the binding sites observed in structures of Src and Lck complexed with a peptide containing the sequence pTyr-Glu-Glu-Ile are much less extensive and in these complexes the mode of peptide binding has been described as a "two-pronged plug" interaction, with the pTyr inserting into a large pocket and the Ile into a separate, smaller pocket. A crystal structure of the amino-terminal SH2 domain of the Syp tyrosine phosphatase (NSyp) in complex with a number of high affinity peptides establishes that an extended

**Fig. 11.** Illustration of the hydrophobic binding sites of the (a) PLCC SH2 (Pascal et al. 1994b), (b) NSyp SH2 (Lee et al. 1994), and (c) Src SH2 domains (Waksman et al. 1992). Blue represents positive and red represents negative electrostatic potential calculated using the program GRASP (Nicholls et al. 1991). The pY1021 and pY1009 peptides (yellow bonds) are shown bound to the PLCC and NSyp SH2 domains, respectively.



binding site is also observed in this system, similar to the PLCC SH2 domain (Lee et al. 1994). A comparison of the PLCC, NSyp, and Src SH2 structures is illustrated in Fig. 11 with focus on the hydrophobic peptide binding sites. Note that similar sites are obtained for the PLCC SH2 and NSyp SH2 domains but that the binding groove is quite distinct in the case of the Src SH2 structure.

Despite the importance of these static 3D structures, it must be recognized that the picture obtained is not complete. Protein molecules are not static in solution and, indeed, the key to a protein's functionality may lie in its dynamic properties. Recently, Shoelson and co-workers (G. Wolf, A. Lynch, M. Chaudhuri, G. Gish, T. Pawson, and S. Shoelson, personal communication) have carried out binding studies where the parent high affinity peptides that bind to a particular SH2 domain were either (i) truncated one residue at a time or (ii) substituted with an alternative amino acid. In both cases, binding affinities were measured and compared with the parent peptide. In the case of the NSyp SH2 domain, it was found that hydrophobic residues at the +5 position (i.e., the position five residues C-terminal to the pTyr) and the +3 position are critical for high affinity binding. Peptides extending only to the +2 position show binding affinities that are reduced by over a factor of 300 relative to parent peptide. These results are expected on the basis of the extended hydrophobic binding groove of the NSyp SH2 domain, which contacts residues on the peptide up to the +5 position. However, a tripeptide centered on the pTyr was found to bind to the PLCC SH2 domain with only a fifteenfold reduction in affinity ( $K_d = 15 \mu\text{M}$ ) relative to the parent peptide (1  $\mu\text{M}$ ). Moreover, truncation of residues at the +2 through +6 positions had significantly smaller effects on binding for the PLCC SH2 domain relative to the NSyp SH2 domain. The results for the PLCC SH2 binding are unexpected given the fact that both the PLCC SH2 and the NSyp SH2 domains have similar extended binding sites.

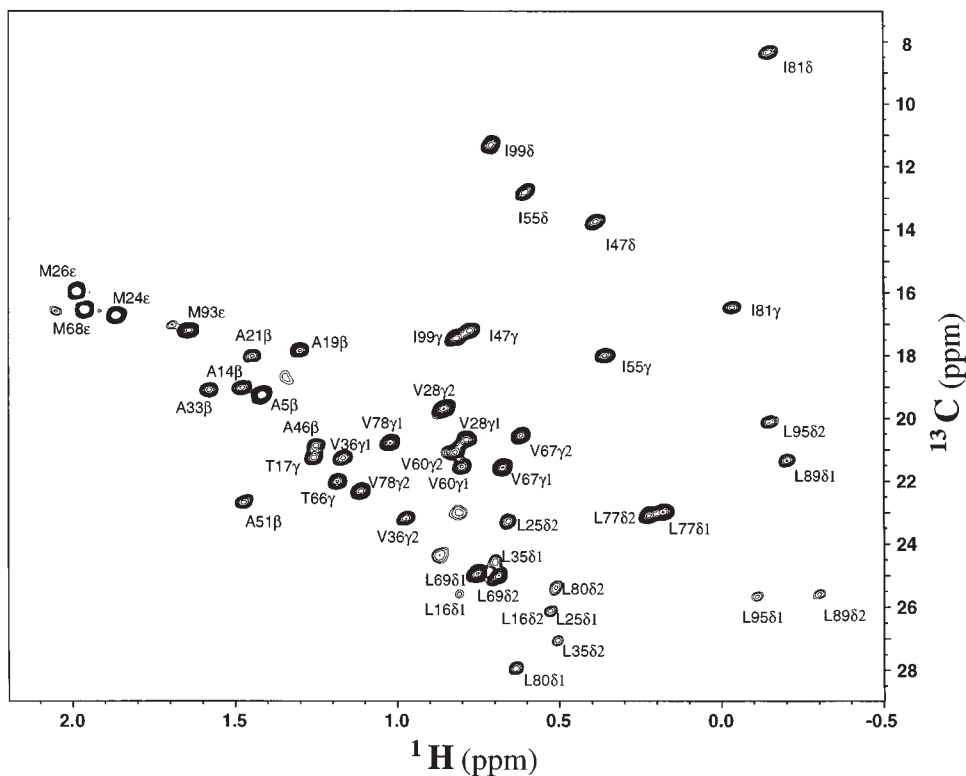
In an effort to understand why the extensive contacts be-

tween the PLCC SH2 domain and peptide residues at the +2 through +6 positions do not confer significant binding energy or specificity, we have undertaken a study of the dynamics of methyl side chains in both the free and complexed forms of the PLCC and NSyp SH2 domains. Molecular dynamics are most often studied using NMR by monitoring spin-relaxation properties of specific nuclei in the molecule. The overall tumbling of the molecule in solution and the internal dynamics result in motion of the individual atoms and many of these atoms have magnetically active nuclei. The motions of these nuclei result in the generation of fluctuating magnetic fields in much the same way that movement of a bar magnet in space creates a time-varying magnetic field. If these magnetic fields fluctuate at frequencies corresponding to the resonance (absorption) frequencies of the nuclei in the system, then these fields restore the signal to its equilibrium state via a process or processes termed spin-relaxation.

In principle, NMR spectroscopy is a powerful technique for probing side-chain dynamics of proteins and a number of studies of methyl dynamics at specific  $^{13}\text{C}$ -labeled sites in proteins have appeared in the literature (Nicholson et al. 1992 and references therein). In practice, however, a number of difficulties with such techniques have emerged. First, only a small subset of the side-chains can be examined in this way. Second,  $^{13}\text{C}$  spin-relaxation methods are hampered by interference (cross correlation) between  $^1\text{H}$ - $^{13}\text{C}$  dipoles in methylene and methyl groups that can result in systematic errors in extracted motional parameters. To circumvent these problems, we have developed a new strategy for studying picosecond–nanosecond side-chain dynamics based on the fractional incorporation of deuterium into uniformly  $^{15}\text{N}$ ,  $^{13}\text{C}$ -labeled proteins (Muhandiram et al. 1995).

In contrast with the relatively recent resurgence of interest in the use of deuteration for high resolution macromolecular NMR studies (discussed above),  $^2\text{H}$  NMR spectroscopy has enjoyed a rich history in the study of molecular dynamics

**Fig. 12.** Two-dimensional contour plot of the constant time ( $^{13}\text{C}, ^1\text{H}$ ) spectrum of the PLCC SH2 domain recorded at 600 MHz. Only signals from  $^{13}\text{CH}_2\text{D}$  methyl groups are observed. Reproduced with permission from Muhandiram et al. (1995).



through measurements of  $^2\text{H}$  relaxation and (or) line shape parameters. The key to the use of deuterium as a probe of molecular dynamics via NMR spin–relaxation lies in the fact that the energy of a deuteron depends critically on its local environment. This interaction (quadrupolar) is well understood and the interpretation of deuterium relaxation data is more straightforward than is the case for relaxation data from many other nuclei. Most  $^2\text{H}$  NMR studies to date have focused to a large extent on the use of liquid crystalline samples or samples in the solid state. In the case of protein applications, these experiments do not provide the necessary resolution to examine the dynamics at many positions in the molecule simultaneously. It is therefore necessary to prepare a large number of samples with labeling at different positions. In principle, solution state measurements can circumvent the problem of resolution, at least for proteins of modest size. However, even in solution, the deuterium lines in a protein are extremely broad. Thus, the experiments that we have developed record the relaxation properties of the deuterons indirectly through measurement of a series of high resolution, constant time  $^{13}\text{C}, ^1\text{H}$  correlation maps where the intensity of the correlations relate to the relevant  $^2\text{H}$  relaxation property,  $T_1$  or  $T_{1\rho}$ . Dynamics information about any labeled site in the molecule can be obtained. To date, we have restricted our analysis to methyl groups because of the excellent resolution and sensitivity in this region of the correlation spectrum. The method allows dynamic information to be extracted from all methyl positions in the molecule simultaneously in a manner that is free from the effects of cross correlation (Yang and Kay 1996a). Figure 12 illustrates the  $^{13}\text{C}–^1\text{H}$  correlation map of the PLCC SH2 do-

main recorded at 600 MHz. Excellent resolution is available in this spectrum and deuterium dynamics data from over 95% of the methyl groups in the protein were measured.

Application of the deuterium relaxation experiments to the PLCC SH2 domain establishes that there is a restriction of motion in the pTyr binding region, which is the site responsible for much of the binding energy. In contrast, the hydrophobic binding site responsible for recognition of sequences C-terminal to the pTyr displays significant ps–ns motional disorder. Surprisingly, certain of the residues of the SH2 domain that line the binding site contacting the +1 through +6 positions of the peptide and make many contacts with the pY1021 peptide are highly flexible (Kay et al. 1996). These results suggest a correlation between motional properties of various groups in the complex and their importance for high affinity binding. In the case of hydrophobic residues lining the binding site, the combination of significant amplitude motions and the steep distance dependence of the van der Waals potential may well result in a substantial decrease in the interaction energy that would otherwise exist in a static site. In contrast with the results obtained on the PLCC SH2 domain, preliminary dynamics studies of the NSyp SH2 domain indicate that the hydrophobic binding interface is more rigid in this system than in the PLCC SH2 – peptide complex; this increased rigidity may explain why hydrophobic interactions in the NSyp SH2 domain are more stabilizing than in the PLCC SH2 domain.

### From protein dynamics to protein thermodynamics

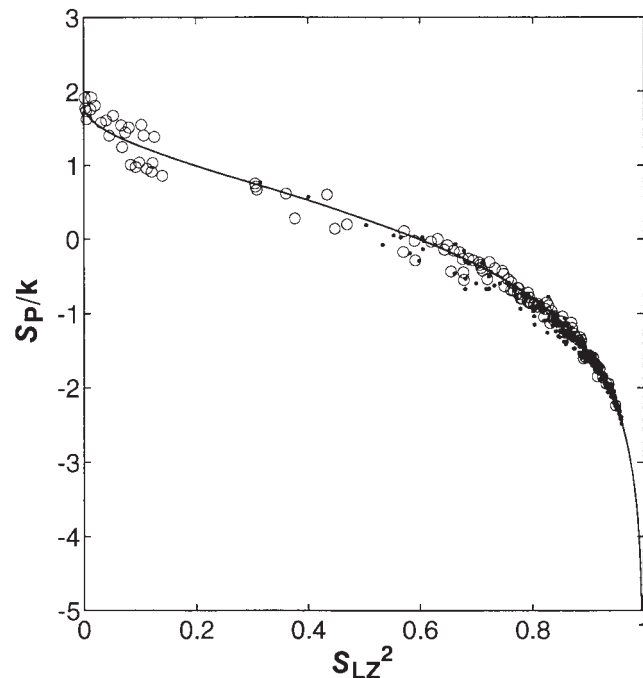
Many biological processes, such as folding and protein-mediated

recognition, involve significant changes in thermodynamics parameters that are often not well understood. For example, although protein–protein interfaces often show interactions involving a large number of residues, it is usually not clear on the basis of the structure which interactions are critical for stabilization of the complex and which play only a marginal role in stability and recognition (Clakson and Wells 1995). A detailed understanding of the energetics of a given biological event is crucial for a complete understanding of stability and function. Experimentally, global thermodynamic values that measure a net change in the system have been measured from optical methods as well as calorimetric approaches (Plum and Breslauer 1995). However, it is difficult to extract information on a per-site basis from these experiments.

As described above, NMR spin–relaxation experiments can provide important insight about molecular dynamics at each site of the molecule. The interpretation of the relaxation parameters provided by such experiments is often accomplished in the context of (i) an order parameter  $S$  that is related to the amplitude of the motion and (ii) correlation times describing the time scale of the dynamics (Lipari and Szabo 1982). Because both the entropy and the order parameter of a given bond vector are related to the distribution of orientations of the vector, it is indeed possible to derive a relationship between changes in order parameters that accompany some molecular transition between states and changes in conformational entropy. Our work in this area (Yang and Kay 1996b) follows closely on a study by Akke et al. (1993), who have related changes in free energy with changes in NMR derived order parameters. Entropy changes, unlike changes in free energy, depend only on the shapes of the potential functions describing the bond motion in the two states and not on the differences in energies between the two states. Therefore, entropy changes are obtained in a more direct manner from NMR relaxation measurements than free energy differences.

In principle, if the potential surface dictating the trajectory of bond vectors in macromolecules were known in detail, it would be a simple matter to derive the correct relationship between the contribution to entropy arising from bond vector motion that is measured in an NMR experiment and the order parameter. The reality is that our knowledge of the energy surface of a complex molecule like a protein is crude at best. With this in mind, we examined a large number of models describing bond vector motion and concluded that the relationship between the measured order parameter and the calculated entropy was very much model dependent. Insight into bond vector motions in proteins can be obtained from molecular dynamics trajectories. A 1.12 ns simulation of fully solvated *E. coli* ribonuclease HI [RNase HI] (Philippopoulos and Lim 1995) was used to determine if any of the models considered provided a reasonable description of bond vector motion. An entropy-order parameter profile was calculated from the backbone N–NH, C $^\alpha$ –C $^\alpha$ H, and side-chain N–NH bond vectors in RNase HI and was compared with the results predicted on the basis of different models. Remarkably, excellent agreement between a model in which the bond vectors are predicted to move within a cone and the molecular dynamics results was obtained as illustrated in Fig. 13. This leads to a simple relationship describing the contribution to the change in entropy arising from a change in bond vector motion as measured in NMR spin–relaxation experiments (Yang and Kay 1996b).

**Fig. 13.** Conformational entropy,  $S_p$ , versus the square of the order parameter,  $S_{LZ}^2$ , calculated from the final 800 ps of a molecular dynamics trajectory of the hydrated protein RNase HI (Philippopoulos and Lim 1995).  $k$  is Boltzmann's constant. Backbone (•) N–NH and C $^\alpha$ –H $^\alpha$  and side chain (o) N–NH bond vectors are included. Reproduced with permission from Yang et al. (1996).



We have applied the entropy-order parameter relationship, derived on the basis of diffusion of bond vectors in a cone, to measure the conformational entropy change associated with a folding transition involving the N-terminal SH3 domain of the *Drosophila* signal transduction protein, drk. Specifically, because the NMR spin–relaxation experiments are sensitive to ps–ns time-scale bond vector motions, the entropy changes calculated reflect the contributions from such rapid motions. It is noteworthy that the magnitude of the entropy changes observed (average entropy change per residue of 12 J·mol $^{-1}$ ·K $^{-1}$ ) is similar to the average entropy change per residue measured for protein folding from a number of different methods,  $\sim$ 14 J·mol $^{-1}$ ·K $^{-1}$  (Doog and Sternberg 1995).

## Conclusions

Recent developments in multidimensional, multinuclear NMR spectroscopy have greatly increased the size range of biomolecules that can be studied by this technology as well as the scope of experimental information available. It is clear that deuteration of proteins can both extend the molecular weight limitations currently imposed on structural studies by NMR as well as provide information about molecular dynamics through the measurement of deuterium relaxation properties. A combination of both structural and dynamical studies promises to provide insight into biological function that static three-dimensional structures alone can not provide.

## Acknowledgements

This research was supported by grants from the Natural Sciences and Engineering Research Council of Canada, the Medical Research Council of Canada, and the National Cancer Institute of Canada with funds from the Canadian Cancer Society. The author is extremely grateful to his mentors, Dr. R.E.D. McClung (University of Alberta), Dr. Brian D. Sykes (University of Alberta), Dr. Jim Prestegard (Yale), Dr. Ad Bax (NIH), and Dr. Dennis Torchia (NIH), and to his many colleagues in Toronto. All of the work in this laboratory benefits from the enthusiastic support of Dr. Julie Forman-Kay. In particular, the SH2 domain project is a collaboration between both of our laboratories as well as the laboratory of Dr. Tony Pawson. The author is also grateful to have had the opportunity of collaborating with his father and it is worth noting that in 1970 he was the recipient of this award as well. The author thanks Drs. Kevin Gardner and Ranjith Muhandiram for assistance with the preparation of figures for this manuscript. Finally, the author expresses his gratitude to Merck Frosst Canada for sponsorship of this award.

## References

Akke, M., Bruschweiler, R., and Palmer, A.G. 1993. NMR order parameters and free energy: an analytical approach and its application to cooperative  $\text{Ca}^{2+}$  binding by calbindin D<sub>9k</sub>. *J. Am. Chem. Soc.* **115**: 9832–9833.

Bax, A. 1994. Multidimensional nuclear magnetic resonance methods for protein studies. *Curr. Opin. Struct. Biol.* **4**: 738–744.

Clackson, T., and Wells, J.A. 1995. A hot spot of binding energy in a hormone-receptor interface. *Science (Washington, D.C.)*, **267**: 383–386.

Crespi, H.L., Rosenberg, R.M., and Katz, J.J. 1968. Proton magnetic resonance of proteins fully deuterated except for <sup>1</sup>H-leucine side chains. *Science (Washington, D.C.)*, **161**: 795–796.

Doog, A.J., and Sternberg, M.J.E. 1995. Sidechain conformational entropy in protein folding. *Protein Sci.* **4**: 2247–2251.

Eck, M.J., Atwell, S.K., Shoelson, S.E., and Harrison, S.C. 1994. Structure of the regulatory domains of the Src-family tyrosine kinase Lck. *Nature (London)*, **368**: 764–769.

Ernst, R.R., Bodenhausen, G., and Wokaun, A. 1987. Principles of magnetic resonance in one and two dimensions. Clarendon Press, Oxford.

Gardner, K.H., Konrat, R., Rosen, M.K., and Kay, L.E. 1996. A (H)C(CO)NH-TOCSY pulse scheme for sequential assignment of protonated methyl groups in otherwise deuterated <sup>15</sup>N, <sup>13</sup>C labeled proteins. *J. Biomol. NMR*, **8**: 351–356.

Gardner, K.H., Rosen, M.K., and Kay, L.E. 1997. Global folds of highly deuterated, methyl-protonated proteins by multidimensional NMR. *Biochemistry*, **36**: 1389–1401.

Grzesiek, S., Anglister, J., Ren, H., and Bax, A. 1993. <sup>13</sup>C line narrowing by <sup>2</sup>H decoupling in <sup>2</sup>H/<sup>13</sup>C/<sup>15</sup>N enriched proteins. Application to triple resonance 4D J correlation of sequential amides. *J. Am. Chem. Soc.* **115**: 4369–4370.

Ikura, M., Clore, G.M., Gronenborn, A.M., Zhu, G., Klee, C.B., and Bax, A. 1992. Solution structure of a calmodulin-target peptide complex by multidimensional NMR. *Science (Washington, D.C.)*, **256**: 632–638.

Janin, J., Miller, S., and Chothia, C. 1988. Surface, subunit interfaces and interior of oligomeric proteins. *J. Mol. Biol.* **204**: 155–164.

Kay, L.E. 1995a. Field gradient techniques in NMR spectroscopy. *Curr. Opin. Struct. Biol.* **5**: 674–681.

Kay, L.E. 1995b. Pulsed field gradient multi-dimensional NMR methods for the study of protein structure and dynamics in solution. *Prog. Biophys. Molec. Biol.* **63**: 277–299.

Kay, L.E., Keifer, P., and Saarinen, T. 1992. Pure absorption gradient enhanced heteronuclear single quantum correlation spectroscopy with improved sensitivity. *J. Am. Chem. Soc.* **114**: 10 663–10 665.

Kay, L.E., Muhandiram, D.R., Farrow, N.A., Aubin, Y., and Forman-Kay, J.D. 1996. Correlation between dynamics and high affinity binding in an SH2 domain interaction. *Biochemistry*, **35**: 361–368.

Keeler, J., Clowes, R.T., Davis, A.L., and Laue, E. 1994. Pulsed field gradients: theory and practice. In *Methods in enzymology, nuclear magnetic resonance. Part C. Vol. 239*. Edited by T.L. James and N.J. Oppenheimer. Academic Press, New York. pp. 145–208.

Lee, C.H., Kominos, D., Jacques, S., Margolis, B., Schlessinger, J., Shoelson, S.E., and Kuriyan, J. 1994. Crystal structures of peptide complexes of the amino-terminal SH2 domain of the Syp tyrosine phosphatase. *Structure*, **2**: 423–438.

LeMaster, D.M., and Richards, F.M. 1988. NMR sequential assignment of *Escherichia coli* thioredoxin utilizing random fractional deuteration. *Biochemistry*, **27**: 142–150.

Lipari, G., and Szabo, A. 1982. Model free approach to the interpretation of nuclear magnetic resonance relaxation in macromolecules. *J. Am. Chem. Soc.* **104**: 4546–4570.

Markley, J.L., Putter, I., and Jardetzky, O. 1968. High resolution nuclear magnetic resonance spectra of selectively deuterated staphylococcal nuclease. *Science (Washington, D.C.)*, **161**: 1249–1251.

Muhandiram, D.R., and Kay, L.E. 1994. Gradient enhanced triple-resonance three-dimensional NMR experiments with improved sensitivity. *J. Magn. Reson. Ser. B*, **103**: 203–216.

Muhandiram, D.R., Yamazaki, T., Sykes, B.D., and Kay, L.E. 1995. Measurement of <sup>2</sup>H T<sub>1</sub> and T<sub>1ρ</sub> relaxation times in uniformly <sup>13</sup>C-labeled and fractionally <sup>2</sup>H-labeled proteins in solution. *J. Am. Chem. Soc.* **117**: 11 536–11 544.

Nicholls, A., Sharp, K.A., and Honig, B. 1991. Protein folding and association: insights from the interfacial and thermodynamic properties of hydrocarbons. *Protein Struct. Funct. Genet.* **11**: 281–296.

Nicholson, L.K., Kay, L.E., Baldisseri, D.M., Arango, J., Young, P.E., Bax, A., and Torchia, D.A. 1992. Dynamics of methyl groups in proteins as studied by proton-detected <sup>13</sup>C NMR spectroscopy. Application to the leucine residues of staphylococcal nuclease. *Biochemistry*, **31**: 5253–5263.

Pascal, S.M., Muhandiram, D.R., Yamazaki, T., Forman-Kay, J.D., and Kay, L.E. 1994a. Simultaneous acquisition of <sup>15</sup>N- and <sup>13</sup>C-edited NOE spectra of proteins dissolved in H<sub>2</sub>O. *J. Magn. Reson. Ser. B*, **103**: 197–201.

Pascal, S.M., Singer, A.U., Gish, G., Yamazaki, T., Shoelson, S.E., Pawson, T., Kay, L.E., and Forman-Kay, J.D. 1994b. Nuclear magnetic resonance structure of an SH2 domain of phospholipase C<sub>γ</sub>1 complexed with a high affinity binding peptide. *Cell*, **77**: 461–472.

Philippopoulos, M., and Lim, C. 1995. Molecular dynamics of *E. coli* ribonuclease H1 in solution: correlation with NMR and X-ray data and insights into biological function. *J. Mol. Biol.* **254**: 771–792.

Plum, G.E., and Breslauer, K.J. 1995. Calorimetry of proteins and nucleic acids. *Curr. Opin. Struct. Biol.* **5**: 682–690.

Rosen, M.K., Gardner, K.H., Willis, R.C., Parris, W.E., Pawson, T., and Kay, L.E. 1996. Selective methyl group protonation of perdeuterated proteins. *J. Mol. Biol.* **263**(5): 627–636.

Schleucher, J., Sattler, M., and Griesinger, C. 1993. Coherence selection by gradients without signal attenuation: application to the three-dimensional HNCO experiment. *Angew Chem. Int. Ed. Engl.* **32**: 1489–1491.

Schleucher, J., Schwendinger, M., Sattler, M., Schmidt, P., Schedletzky, O., Glaser, S.J., Sorensen, O.W., and Griesinger, C. 1994. A general enhancement scheme in heteronuclear multidimensional NMR employing pulsed field gradients. *J. Biomol. NMR*, **4**: 301–306.

Shan, X., Gardner, K.H., Muhandiram, D.R., Rao, N.S., Arrowsmith, C.H., and Kay, L.E. 1996. Assignment of  $^{15}\text{N}$ ,  $^{13}\text{C}^\alpha$ ,  $^{13}\text{C}^\beta$  and HN resonances in an  $^{15}\text{N}$ ,  $^{13}\text{C}$ ,  $^2\text{H}$  labeled 64 kDa Trp repressor-operator complex using triple resonance NMR spectroscopy and  $^2\text{H}$  decoupling. *J. Am. Chem. Soc.* **118**: 6570–6579.

Waksman, G., Komino, D., Robertson, S.C., Pant, N., Baltimore, D., Birge, R.B., Cowburn, D., Hanafusa, H., Mayer, B.J., Overduin, M., Resh, M.D., Rios, C.B., Silverman, L., and Kuriyan, J. 1992. Crystal structure of the phosphotyrosine recognition domain SH2 of v-src complexed with tyrosine-phosphorylated peptides. *Nature (London)*, **358**: 646–653.

Wuthrich, K. 1986. NMR of proteins and nucleic acids. Wiley, New York.

Yang, D., and Kay, L.E. 1996a. The effects of cross correlation and cross relaxation on the measurement of deuterium  $T_1$  and  $T_{1\text{p}}$  relaxation times in  $^{13}\text{CH}_2\text{D}$  spin systems. *J. Magn. Reson. Ser. B*, **110**: 213–218.

Yamazaki, T., Lee, W., Revington, M., Mattiello, D.L., Dahlquist, F.W., Arrowsmith, C.H., and Kay, L.E. 1994a. An HNCA pulse scheme for the backbone assignment of  $^{15}\text{N}$ ,  $^{13}\text{C}$ ,  $^2\text{H}$  labeled proteins: application to a 37-kDa trp-repressor-DNA complex. *J. Am. Chem. Soc.* **116**: 6464–6465.

Yamazaki, T., Lee, W., Arrowsmith, C.H., Muhandiram, D.R., and Kay, L.E. 1994b. A suite of triple resonance NMR experiments for the backbone assignment of  $^{15}\text{N}$ ,  $^{13}\text{C}$ ,  $^2\text{H}$  labeled proteins with high sensitivity. *J. Am. Chem. Soc.* **116**: 11 655 – 11 666.

Yang, D., and Kay, L.E. 1996b. Contributions to conformational entropy arising from bond vector fluctuations measured from NMR-derived order parameters: application to protein folding. *J. Mol. Biol.* **263**(2): 369–382.

Yu, H., and Schreiber, S.L. 1994. Signaling an interest. *Nature Struct. Biol.* **1**: 417–420.

Zhang, H., Zao, D., Revington, M., Lee, W., Jia, X., Arrowsmith, C.H., and Jardetzky, O. 1994. The solution structure of the trp repressor-operator DNA complex. *J. Mol. Biol.* **229**: 735–746.

## Notes about the author

This article is based on the Merck Frosst Award Lecture of the Canadian Society of Biochemistry and Molecular and Cellular Biology presented by Dr. Lewis E. Kay at the 39th Annual Meeting of the Canadian Federation of Biological Societies in London, June 19–22, 1996. Dr. Kay was born and raised in Edmonton, Alberta, and obtained his bachelor's degree at the University of Alberta in Edmonton. He completed his Ph.D. in the Chemistry Department at Yale University in New Haven under the supervision of Dr. Jim Prestegard working on "NMR of biomolecules in solution." After his Ph.D., he did postdoctoral work in the laboratory of Chemical Physics at NIH in Bethesda on "Multi-dimensional NMR of proteins" with Dr. Ad Bax. After completing his postdoctoral studies, he went to Toronto. Since 1992 he has been Professor in the Departments of Medical Genetics, Biochemistry, and Chemistry at the University of Toronto.

## Notes sur l'auteur

Cet article est basé sur la conférence d'acceptation du prix Merck Frost de la Société canadienne de biochimie et biologie moléculaire et cellulaire qui a été décerné au Dr Lewis E. Kay lors du 39e congrès annuel de la Fédération canadienne des sociétés de biologie, tenu à London, Ontario, du 19 au 22 juin 1996. Dr Kay est né et a grandi à Edmonton, Alberta. Il a obtenu un B.Sc. de l'Université de l'Alberta à Edmonton. Puis, il a étudié la "RMN des molécules biologiques en solution" sous la direction du Dr Jim Prestegard, au cours de son programme de doctorat au Département de chimie de l'Université Yale de New Haven, Conn. Après avoir obtenu un Ph.D., il a fait un stage postdoctoral pour étudier la "RMN multidimensionnelle des protéines" avec le Dr Ad Bax, au Laboratoire de chimie physique du NIH à Bethesda. Il est allé à Toronto après son stage postdoctoral. Depuis 1992, il est professeur aux Départements de génétique médicale, de biochimie et de chimie de l'Université de Toronto.